CCL9/CCR1 induces myeloid-derived suppressor cell recruitment to the spleen in a murine H22 orthotopic hepatoma model

BAOHUA LI[1,2], SHU ZHANG[3], NA HUANG[1], HAIYAN CHEN[1], PEIJUN WANG[3], JUN YANG[4] and ZONGFANG LI[2,3]

[1]Core Research Laboratory; [2]National & Local Joint Engineering Research Center of Biodiagnosis and Biotherapy; Departments of [3]General Surgery and [4]Pathology, The Second Affiliated Hospital, College of Medicine, Jiaotong University, Xi'an, Shaanxi 710004, P.R. China

Received March 7, 2018; Accepted October 8, 2018

DOI: 10.3892/or.2018.6809

Abstract. Myeloid-derived suppressor cells (MDSCs) are the major negative regulators of immune responses and expand in numerous tumor models. They contribute to tumor progression and metastasis, and are involved in limiting the effects of cancer immunotherapy. To selectively target MDSCs, it is required to understand the molecular mechanisms that drive MDSC expansion. The mechanisms of their accumulation in tumor tissue have been extensively studied, while the mechanisms of their expansion in lymphoid organs have been rarely explored. The spleen is the largest lymphoid organ in the human body. A previous study by our group reported that a negative immune status in the spleen facilitated tumor growth, with MDSCs being the major immunosuppressive cells. In the present study, a murine H22 orthotopic hepatoma model was established and the mechanisms of splenic MDSC accumulation were studied, including MDSC proliferation, apoptosis and chemotaxis. The proliferation and apoptosis of splenic MDSCs did not differ between normal and tumor-bearing (TB) mice. Cytokine array and ELISA of splenic tissues indicated elevated chemokine (C-C motif) ligand 9 (CCL9) levels in TB mice. Furthermore, splenic macrophages were able to secrete CCL9. Flow cytometric analysis revealed that splenic MDSCs from TB mice also overexpressed C-C motif chemokine receptor 1 (CCR1), the receptor for CCL9. Taken together, the present results indicate that CCL9 secreted by splenic macrophages induces a CCR1-dependent accumulation of MDSCs in the spleen in a murine H22 hepatoma model.

Correspondence to: Professor Zongfang Li, National & Local Joint Engineering Research Center of Biodiagnosis and Biotherapy, The Second Affiliated Hospital, College of Medicine, Jiaotong University, 157 Xi Wu Road, Xi'an, Shaanxi 710004, P.R. China
E-mail: lzf2568@mail.xjtu.edu.cn

Key words: spleen, myeloid-derived suppressor cells, hepatoma, H22, chemokine (c-c motif) ligand 9, C-C motif chemokine receptor 1

Introduction

Myeloid-derived suppressor cells (MDSCs) form a heterogenous population that consists of myeloid progenitor cells, immature macrophages, immature granulocytes and immature dendritic cells (DCs). The phenotype of MDSCs in mice is granulocyte receptor 1 $(Gr\text{-}1)^{+}CD11b^{+}$. In the steady state, MDSCs have no inhibitory activity and are mostly present in the bone marrow. The percentage of MDSCs is only 2-4% in the spleen, and they are absent from the lymph nodes in mice. In tumor hosts, MDSCs accumulate in lymphatic organs and tumor tissue, and they produce a large amount of immune-inhibitory factors, including arginase I, inducible nitric oxide synthase and reactive oxygen species, which inhibit T-cell immune responses (1-3), induce regulatory T-cell production, suppress natural killer (NK) cell functions, and affect cytokine production and secretion by macrophages. Furthermore, MDSCs can facilitate epithelial-mesenchymal transition, angiogenesis and metastasis (2,4-6).

The spleen is the largest immune organ, containing nearly 25% of the body's immune cells. It has a vital role in the immune response to tumors, and splenic NK cells and T cells exert important anti-tumor functions (7-10). However, the spleen is also a reservoir of precursor monocytes and granulocytes, which may be mobilized to the tumor tissue and differentiate into tumor-associated macrophages (TAM) and neutrophils (TAN) that promote tumor progression. Splenectomy has been indicated to markedly reduce TAM and TAN responses, thus retarding tumor growth (11). A previous study by our group identified an immune-suppressive status in the spleen of a H22 orthotopic hepatoma mouse model. MDSCs were the major inhibitory cells causing the immunosuppression in the spleen (12). Similarly, Levy *et al* (13) reported that the spleen may be a reservoir of MDSCs and that splenectomy may reduce the percentage of MDSCs in peripheral blood and tumor tissue.

To date, numerous studies have reported on the mechanisms of MDSC accumulation in tumor tissue, and the factors involved include chemokines, inflammatory factors, colony-stimulating factor and complements (14-16). Tumor-derived chemokines, including C-C motif chemokine ligand (CCL)2, CCL5, CCL21 and C-X-C motif ligand (CXCL)8 were able to recruit MDSCs

to the tumor tissue, while blocking of these chemokines or their receptors reduced the number of MDSCs at the tumor sites and inhibited tumor growth (17-23). The accumulation of MDSCs in the tumor may also be regulated by inflammatory environmental factors, including interleukin (IL)-1β, IL-6, prostaglandin E2, S100 calcium-binding protein A8/9 and tumor necrosis factor (24-28).

By contrast, few studies have assessed MDSC accumulation in the spleen under pathological conditions. In the murine MCA203 fibrosarcoma model, nestin-positive splenocytes were able to secrete CCL2 that attracted MDSCs to the spleen in a CCR2-dependent manner (29). The spleen is the primary site of immune responses, and its immune status influences tumor growth. Therefore, it is important to explore the mechanisms of MDSC localization and kinetics in the spleen under pathological conditions. This may facilitate the identification of novel factors and pathways involved in MDSC accumulation in the spleen that may have a role in the contribution of MDSCs to tumor progression. These factors and pathways may be novel targets in immune therapy to block MDSCs in order to suppress tumor growth.

In the present study, the mechanisms of MDSC accumulation in the spleen of tumor-bearing (TB) mice were explored. MDSC proliferation, apoptosis and the expression of cytokines in the spleen were assessed. Chemokines upregulated in TB mice were validated and their cellular origin was identified.

Materials and methods

Cell culture. The H22 murine hepatoma cell line was purchased from the China Center for Type Culture Collection (Wuhan, China). The cells were cultured in RPMI-1640 medium (HyClone; GE Healthcare, Little Chalfont, UK) supplemented with 10% fetal calf serum (HyClone; GE Healthcare) and 1% penicillin/streptomycin (HyClone; GE Healthcare). The cells were grown at 37˚C in an atmosphere containing 5% CO_2.

Mice. A total of 96 female BALB/c mice (age, 6-8 weeks; weight, 20-25 g) were purchased from the animal center of Xi'an Jiaotong University (Xi'an, China). The mice were housed under specific pathogen-free conditions at the animal facility under a 12-h light/dark cycle and free access to food and water. All animal procedures complied with the Guide for the Care and Use of Laboratory Animals [National Institutes of Health (NIH); publication from 1996] and were approved by the Xi'an Jiaotong University Animal Care and Use Committee (Xi'an, China).

Orthotopic mouse model of hepatocellular carcinoma. Mice were intraperitoneally injected with 10^6 H22 cells (at the concentration of 10^7 cells/ml in saline). After 12 days, ascites fluid containing floating tumor cells was collected from these mice, which was centrifuged at 300 x g for 5 min at 4˚C to retrieve the cells, which were washed twice with saline. These cells were subsequently injected under the capsule of the left liver lobe of each mouse (2 x10^5 tumor cells at the concentration of 10^7 cells/ml). Four days later, white tumor nodules had formed on the liver, indicating the successful generation of the H22 hepatoma model.

Generation of single-cell suspensions of splenocytes. Mice were sacrificed and the spleens were collected at one, two and three weeks after tumor inoculation. Spleens were dissociated into single-cell suspensions with the gentleMACS Dissociator (Miltenyi Biotech, Bergisch Gladbach, Germany) in the buffer [0.01 mol/l PBS, 0.5% bovine serum albumin (Amresco, Solon, OH, USA) and 2 mmol/l EDTA], using the C tube and the 'm_spleen_01' program according to the manufacturer's protocols. Subsequently, the cell suspensions were centrifuged at 300 x g for 30 sec at room temperature. Next, the splenocytes suspensions were strained through a 70-μm mesh to remove clumps and generate single-cell suspensions.

Flow cytometric analysis. The ammonium-chloride-potassium lysis buffer (0.15 mol/l NH_4Cl, 1 mmol/l $KHCO_3$ and 0.1 mmol/l EDTA, pH 7.2) was added to the splenocytes to remove red blood cells. Subsequently, the cells were washed twice with PBS. Cells (10^6) were incubated with anti-CD16/CD32 (cat. no. 101302; 10 μg/ml; BioLegend, San Diego, CA, USA) for 10 min at 4˚C to prevent non-specific labeling of surface receptors. Next, cells were incubated with monoclonal antibodies, including anti-mouse granulocyte receptor 1 (Gr-1)-fluorescein isothiocyanate (FITC) (cat. no. 108405), anti-mouse Ly6G-FITC (cat. no. 127605), anti-mouse Ly6C-phyco erythrin (PE) (cat. no. 128007), anti-mouse CD11b-all ophycocyanine (APC)-(cyanine)Cy7 (cat. no. 101226), anti-mouse C-C motif chemokine receptor 1 (CC R1)-APC (cat. no. 152503) (all from BioLegend; 2.5 μg/ml dilution), anti-mouse CD11b-PE (cat. no. 12-0112; 0.6 μg/ml; eBioscience, San Diego, CA, USA), anti-mouse Fas-APC (cat. no. 17-0951; 10 μg/ml; eBioscience) and their corresponding isotype antibodies, including FITC rat immunoglobulin (Ig)G2b, κ (cat. no. 400605); FITC rat IgG2a, κ (cat. no. 400505); PE rat IgG2c, κ (cat. no. 400707); APC/Cy7 rat IgG2b, κ (cat. no. 400623); APC rat IgG2b, κ (cat. no. 400611) (all from BioLegend; 2.5 μg/ml dilution); PE rat IgG2b, κ (cat. no. 12-4031; 0.6 μg/ml); APC mouse IgG1, κ (cat. no. 17-4714; 10 μg/ml) (both from eBioscience) as the control for 30 min at 4˚C in the dark. Following washing, the cells were analyzed using a FACSCanto instrument with FACSDiva 7.0 software (BD Biosciences, Franklin Lakes, NJ, USA).

To assess splenic MDSC proliferation, splenic cell suspensions were stained with anti-mouse Gr-1-FITC and anti-mouse CD11b-PE antibodies for 30 min at 4˚C, followed by incubation with cold 70% ethanol (precooled to -20˚C; added in a drop-wise manner to the cells while vortexing) at -20˚C for 1 h. Subsequently, the cells were washed three times, stained with anti-mouse Ki-67-APC antibody (cat. no. 652405; 2.5 μg/ml; BioLegend) for 30 min at 4˚C in the dark, washed and analysed with a flow cytometer.

To assess splenic MDSC apoptosis, splenic cell suspensions were stained with anti-mouse Gr-1-FITC and anti-mouse CD11b-PE, followed by Annexin V-APC (cat. no. 640920; BioLegend) and 7-aminoactinomycin D (7-AAD; cat. no. 420403; 2.5 μg/ml; BioLegend). In brief, 10^6 cells were washed twice and re-suspended in Annexin V binding buffer (cat. no. 422201; BioLegend). Next, 5 μl Annexin V-APC

and 5 μl 7-AAD were added to the cells. Cells were incubated for 15 min at 4˚C in the dark, re-suspended in 400 μl binding buffer and analyzed using a FACSCanto II flow cytometer (BD Biosciences) within 1 h.

Fluorescence-activated sorting of splenic macrophages. To isolate splenic macrophages, single-cell suspensions of splenocytes were first incubated with anti-mouse CD16/32 antibody (cat. no. 101302; 10 μg/ml; BioLegend) for 10 min at 4˚C to prevent non-specific labeling of surface receptors, followed by incubation with monoclonal antibodies, including anti-mouse F4/80-PE and (cat. no. 123109; 10 μg/ml; BioLegend) anti-mouse CD11b-APC-Cy7 (cat. no. 101226; 2.5 μg/ml; BioLegend), for 30 min at 4˚C in the dark. Cells were washed twice and F4/80$^+$CD11b$^+$ double-positive cells were isolated with a FACSAria II instrument (BD Biosciences). The purity of the sorted macrophages was verified by flow cytometry (FACSAria II; BD Biosciences).

Cytokine array. The concentrations of cytokines in the spleens of normal and TB mice were quantified using the Mouse Cytokine Array G3 (cat. no. AAM-CYT-G3-4; RayBiotech, Norcross, GA, USA) according to the manufacturer's protocols. After all of the procedure steps, the chip was scanned with an Axon GenePix scanner (GenePix 4000B; Axon Instruments, Inc., San Jose, CA, USA). Protein array data were annotated and processed with GenePix Pro 6.0 software (Molecular Devices, LLC, Sunnyvale, CA, USA). The expression levels (fluorescent signal intensities) of each cytokine were calculated by subtracting the mean absorbance of the blank sample, with normalization to a positive control.

ELISA. The levels of murine CCL9 and CXCL2 in the spleens of normal and TB mice were measured using ELISA kits (cat. nos. F111602 and F1117; Westang, Shanghai, China). Assays were performed in duplicate according to the manufacturer's protocols.

Reverse transcription-quantitative polymerase chain reaction (RT-qPCR). For analysis of CCL9 gene expression, total RNA was extracted from the isolated splenic macrophages using TRIzol reagent (Thermo Fisher Scientific, Inc., Waltham, MA, USA) according to the manufacturer's instructions. Complementary (c)DNA was synthesized using the PrimeScript™ RT reagent kit with a genomic DNA eraser (cat. no. RR047A, Takara Bio, Inc., Otsu, Japan). Real-time PCR was performed using SYBR® Premix Ex Taq™ II (Tli RNaseH Plus) kit (cat. no. RR820A, Takara Bio, Inc.) in a 20-μl reaction system, including 10 μl Premix Ex Taq II (Takara Bio, Inc.), 0.4 μl 5-carboxy rhodamine X reference dye II (Takara Bio, Inc.), 0.8 μl of 0.4 μM forward primer and 0.8 μl of 0.4 μM reverse primer, 2 μl cDNA (resembling the transcription product of 50 ng RNA) and 6 μl distilled water. The following primers were used: CCL9 FP, 5'-CCC TCTCCTTCCTCATTCTTACA-3' and RP, 5'-AGTCTT GAAAGCCCATGTGAAA-3'; GAPDH FP, 5'-AGGTCG GTGTGAACGGATTTG-3' and RP, 5'-TGTAGACCATGT AGTTGAGGTCA-3'. Amplifications of CCL9 and GAPDH transcripts were performed during 40 PCR cycles using the ABI 7500 fast real-time PCR system (Applied Biosystems; Thermo Fisher Scientific, Inc.). The initial denaturation step was at 95˚C for 30 sec. Each PCR amplification cycle included a denaturation step at 95˚C for 5 sec, and a primer annealing and elongation step at 60˚C for 30 sec. The expression levels were calculated as the relative cDNA content normalized to GAPDH expression ($2^{-\Delta\Delta Cq}$ method) (30). Three independent replicates were performed.

Statistical analysis. Values are expressed as the mean ± standard deviation. Data were analyzed with Prism 5 software (GraphPad Software, Inc., La Jolla, CA, USA). Student's t-test was used to compare the difference between the two groups. For more than two groups, one-way ANOVA followed by Dunnett's test was performed. $P<0.05$ was considered to indicate a statistically significant difference.

Results

H22 tumor induces accumulation of MDSCs in the spleen. The murine H22 orthotopic HCC model was established and it was determined whether the development of H22 tumors was associated with an increased number of MDSCs in the spleen. The percentage of splenic MDSCs increased significantly in TB mice compared with that in normal mice at week 1 (6.82±2.92 vs. 3.44±0.60%, $P<0.05$), week 2 (43.20±11.03 vs. 4.90±0.90%, $P<0.001$) and week 3 (13.28±4.66 vs. 3.42±0.48%, $P<0.001$) post-tumor inoculation, with the greatest difference observed at week 2 (Fig. 1). These results suggest that a H22 tumor may induce the accumulation of CD11b$^+$Gr-1$^+$ cells in the spleen *in vivo*.

Accumulation of MDSCs in the spleen is not associated with their proliferation and apoptosis. It was investigated whether the accumulation of splenic MDSCs in TB mice resulted from their increased proliferation and/or reduced apoptosis. First the proliferation status of splenic MDSCs was assessed by staining for Ki-67, a marker of cell proliferation. The percentage of Ki-67$^+$ splenic MDSCs was not significantly different between TB mice and normal mice at any of the time-points. The mean fluorescent intensity (MFI) of Ki-67 in splenic MDSCs was also not significantly different between TB mice and normal mice (Fig. 2).

Next, the apoptosis of splenic MDSCs was assessed. No difference in the amount of total (AnnexinV$^+$) apoptotic MDSCs was identified between TB and normal mice at weeks 1, 2 and 3 post-tumor inoculation (Fig. 3). Fas protein is an apoptotic protein expressed on the cell surface, and therefore, Fas expression on the splenic MDSCs was also assessed. Neither the percentage of Fas$^+$ splenic MDSCs nor the MFI of Fas in splenic MDSCs was different between TB mice and normal mice at any of the time-points assessed (Fig. 4).

These results indicate that the accumulation of MDSCs in the spleen was not associated with their proliferation or apoptosis.

Accumulation of splenic MDSCs in TB mice is associated with increases in the level of splenic CCL9. The accumulation of splenic MDSCs in TB mice may be caused by their chemotaxis to the spleen (29). To identify the factors involved, a protein chip assay was then performed for the simultaneous

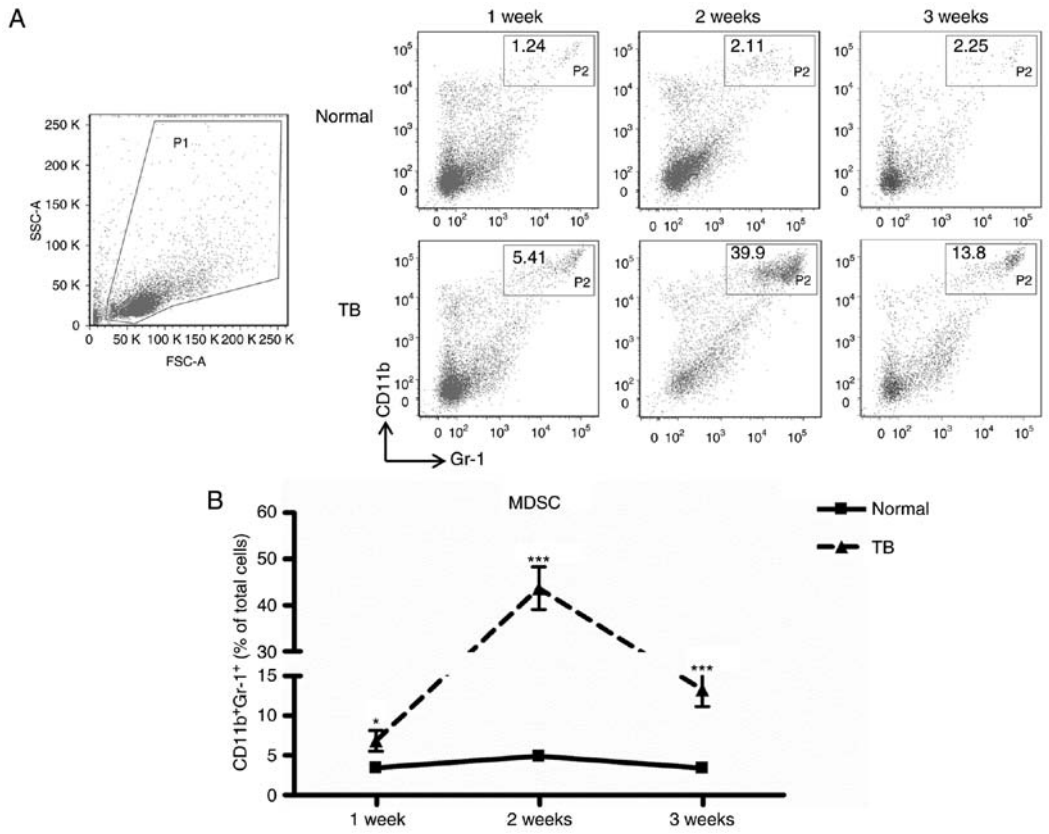

Figure 1. MDSCs accumulate in the spleen during tumor growth. Single-cell suspensions of splenocytes were prepared and stained with anti-mouse-Gr-1 monoclonal antibody conjugated with FITC and anti-mouse CD11b monoclonal antibody conjugated with PE, and analyzed by flow cytometry. (A) Representative fluorescence-assisted cell sorting plots of splenocyte preparations. A live gate P1 was set in the FSC/SSC plot. Subsequently, the populations of CD11b-PE and Gr-1-FITC cells were displayed in dot plots. (B) The percentage of splenic MDSCs ($Gr\text{-}1^+CD11b^+$, gate P2 within live gate) in H22 hepatoma mice (▲) and normal mice (■) at weeks 1, 2 and 3 post-tumor inoculation (n=6); Values are expressed as the mean ± standard deviation. $^*P<0.05$ and $^{***}P<0.001$ compared with normal mice. TB, tumor-bearing; MDSCs, myeloid-derived suppressor cells; FITC, fluorescein isothiocyanate; PE, phycoerythrin; SSC, side scatter; FSC, forward scatter; Gr-1, granulocyte receptor 1.

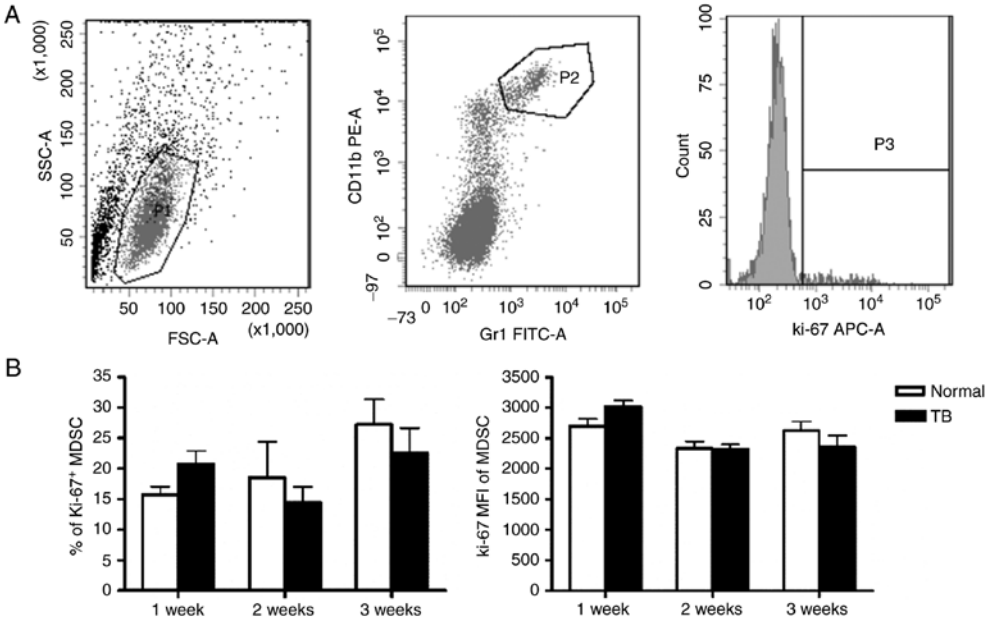

Figure 2. Accumulation of splenic MDSCs in H22 hepatoma mice is not associated with their proliferative status. Single-cell suspensions of splenocytes were stained with anti-mouse Gr-1 monoclonal antibody conjugated with FITC and anti-mouse CD11b monoclonal antibody conjugated with PE, followed by permeabilization with 70% ethanol and staining with anti-mouse Ki-67 antibody conjugated with APC. (A) Representative flow cytometry plots and gating strategy. A live gate P1 was set in the FSC/SSC plot and $CD11b^+/Gr\text{-}1^+$ were included in the further analysis with gate P2. Subsequently, the selected cells were displayed in a histogram for Ki-67-APC. (B) The percentage of $Ki\text{-}67^+$ MDSCs (left panel) and the MFI of Ki-67 in MDSCs (right panel) in H22 hepatoma and normal mice (n=6). Values are expressed as the mean ± standard deviation. TB, tumor-bearing; APC, allophycocyanine; MDSCs, myeloid-derived suppressor cells; FITC, fluorescein isothiocyanate; PE, phycoerythrin; SSC, side scatter; FSC, forward scatter; Gr-1, granulocyte receptor 1; MFI, mean fluorescent intensity.

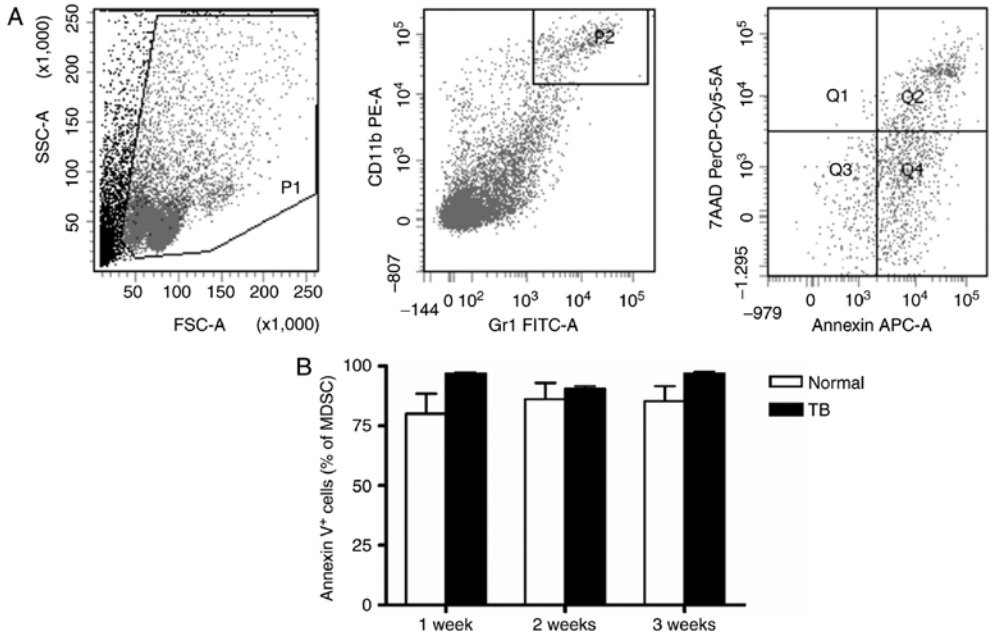

Figure 3. Accumulation of splenic MDSCs in H22 hepatoma mice is not caused by alterations in their apoptotic rate. Single-cell suspensions of splenocytes were stained with anti-mouse Gr-1 monoclonal antibody conjugated with FITC and anti-mouse CD11b monoclonal antibody conjugated with PE, followed by staining with anti-mouse AnnexinV antibody conjugated with APC and viability dye 7-AAD. (A) Representative flow cytometry plots and gating strategy. A live gate P1 was set in the FSC/SSC plot and CD11b$^+$/Gr-1$^+$ cells were included in the further analysis with gate P2. Subsequently, the selected cells were displayed in histograms for Annexin-APC or 7-AAD. Annexin V$^+$/7-AAD$^-$ indicates cells in early apoptosis and Annexin V$^+$/7-AAD$^+$ indicates cells in late apoptosis. (B) Total apoptotic MDSC populations (AnnexinV$^+$) in TB and normal mice are presented. Values are expressed as the mean ± standard deviation (n=6). TB, tumor-bearing; APC, allophycocyanine; MDSCs, myeloid-derived suppressor cells; FITC, fluorescein isothiocyanate; PE, phycoerythrin; SSC, side scatter; FSC, forward scatter; Gr-1, granulocyte receptor 1; 7-AAD, 7-amino actinomycin D; PerCP, peridinin chlorphyll protein; Cy, cyanine.

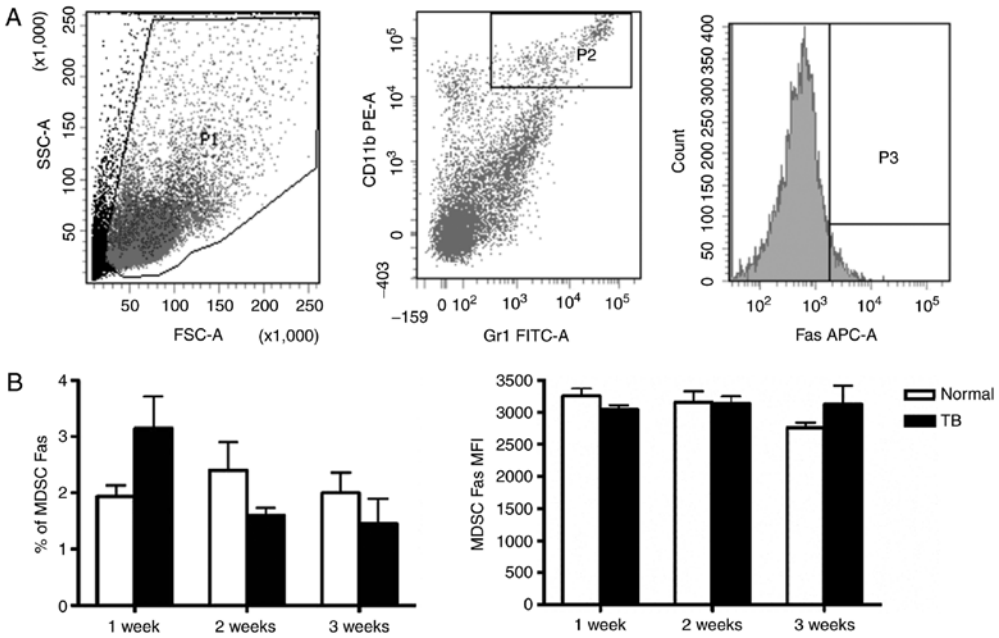

Figure 4. Mice with hepatoma and normal mice do not exhibit any difference in the expression of apoptotic protein Fas in splenic MDSCs. Single-cell suspensions of splenocytes were stained with anti-mouse Gr-1 antibody conjugated with FITC, anti-mouse CD11b antibody conjugated with PE and anti-mouse Fas antibody conjugated with APC. (A) Representative flow cytometry plots and gating strategy. A live gate P1 was set in the FSC/SSC plot and CD11b$^+$/Gr-1$^+$ cells were included in a further analysis with gate P2. Subsequently, the selected cells were displayed in a histogram for Fas-APC. (B) The percentage of Fas$^+$ MDSCs (left panel) and the MFI of Fas in MDSCs (right panel) in H22 hepatoma and normal mice. Values are expressed as the mean ± standard deviation (n=6). TB, tumor-bearing; APC, allophycocyanine; MDSCs, myeloid-derived suppressor cells; FITC, fluorescein isothiocyanate; PE, phycoerythrin; SSC, side scatter; FSC, forward scatter; Gr-1, granulocyte receptor 1; MFI, mean fluorescent intensity.

detection of 62 cytokines in the spleen of TB and untreated mice at weeks 1, 2 and 3 post-tumor inoculation (Fig. 5A). At certain time-points, the fluorescent signals of 11 cytokines were higher and those of 8 cytokines were lower in TB mice

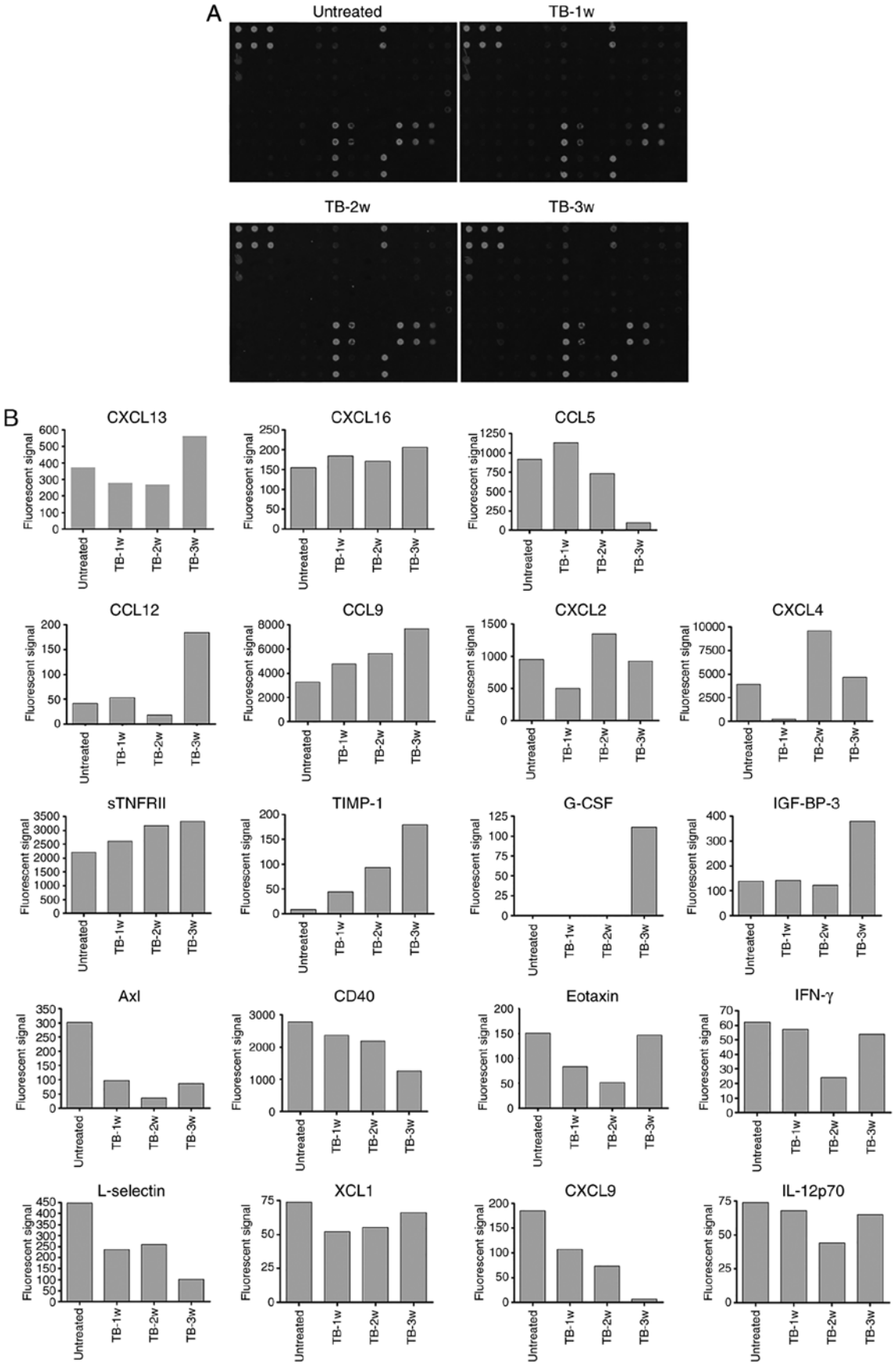

Figure 5. Differential expression of 62 cytokines in the spleen of H22 hepatoma and normal mice. A RayBiotech mouse cytokine antibody array was used to compare the expression of 62 cytokines in the splenic tissues of untreated and TB mice. (A) Mouse cytokine antibody array membranes. (B) Quantification of A. The upregulated (upper part) and downregulated (lower part) cytokines in the spleen of TB mice compared with untreated mice. Among the upregulated cytokines, seven chemokines are indicated by rectangles. TB, tumor-bearing; 1w, 1 week; G-CSF, granulocyte-colony stimulating factor; IGFBP3, insulin-like growth factor-binding protein 3; CCL12, chemokine (C-C motif) ligand 12; CXCL2, chemokine (C-X-C motif) ligand 2; sTNFR, soluble tumor necrosis factor receptors; TIMP1, tissue inhibitors of metalloproteinase 1; IFN, interferon; IL, interleukin; XCL1, chemokine (C motif) ligand.

Table I. Upregulated chemokines in spleen of H22 hepatoma mice. A total of 62 cytokines were detected in spleen tissue of untreated and TB mice at weeks 1, 2 and 3 post-tumor inoculation using a mouse cytokine antibody array.

	Fluorescent signal intensity (normalized to positive control)				
Abbreviation	Untreated	TB-1w	TB-2w	TB-3w	Chemotactic cells
CXCL13	374	282	270	563	B
CXCL16	155	184	171	206	T, NKT
CCL5	916	1132	729	91	T, eosinophils, basophils
CCL12	42	53	18	184	Eosinophils, monocytes, lymphocytes
CCL9	3298	4770	5644	7677	DC
CXCL2	955	502	1343	926	Polymorphonuclear leukocytes
CXCL4	3907	256	9609	4638	Neutrophils, monocytes, fibroblasts

DC, dendritic cells, NKT, natural killer T-cells; TB, tumor-bearing; 1w, 1 week; CXCL13, chemokine (C-X-C motif) ligand 13; CCL5, chemokine (C-C motif) ligand 5.

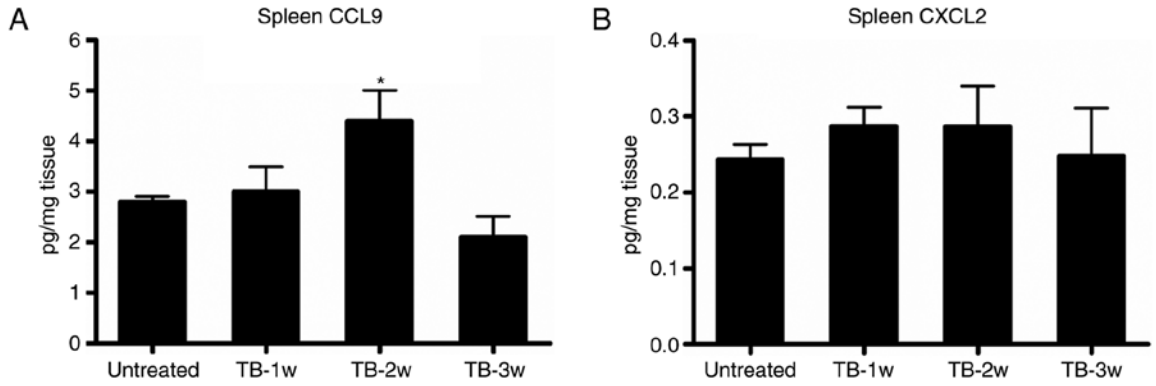

Figure 6. Accumulation of splenic MDSCs is caused by increases of CCL9 levels in the spleens of H22 hepatoma mice. The expression of (A) CCL9 and (B) CXCL2 in the spleen tissues of untreated and TB mice was determined using ELISA. The spleen tissues were harvested at week 1, week 2 and week 3 post-tumor inoculation and lysed. Lysates were clarified and the protein concentration was measured using ELISAs. Values are expressed as the mean ± standard deviation (pg/mg of chemokine/splenic tissue, n=5). *P<0.05 compared with untreated mice. TB, tumor-bearing; 1w, 1 week; CCL9, chemokine (C-C motif) ligand 9; CXCL2, chemokine (C-X-C motif) ligand 2.

compared with those in untreated mice. Among the upregulated cytokines, there were 7 chemokines: Chemokine (C-X-C motif) ligand 13 (CXCL13), CXCL16, chemokine (C-C motif) ligand 5 (CCL5), CCL12, CCL9, CXCL2 and CXCL4 (Fig. 5B). However, two of them, CXCL16 and CCL12, were only expressed at low levels and one of them, CXCL13, also known as B lymphocyte chemoattractant, is a chemotactic factor for B lymphocytes. Another chemokine, CCL5, is a chemotactic factor for T cells, eosinophils and basophils. CXCL4 has been reported to negatively control the amount of MDSCs (31), as well as to inhibit angiogenesis and tumor growth (32,33). Therefore, its elevated expression was not correlated with the accumulation of MDSCs (Table I). Subsequently, the role of CCL9 and CXCL2 in MDSC accumulation in the spleen of TB mice was further investigated.

The expression of CCL9 was significantly higher in the spleen of TB mice compared with that in untreated mice at week 2 post-tumor inoculation (Fig. 6A), while there was no significant difference in the expression of CXCL2 at any of the time-points assessed (Fig. 6B). Next, it was determined whether splenic MDSCs expressed CCR1, the receptor for CCL9. It was revealed that splenic MDSCs isolated from TB mice and normal mice expressed CCR1. Furthermore, granulocyte-like MDSCs (G-MDSCs, $CD11b^{+}ly6G^{+}ly6C^{low}$) and monocyte-like MDSCs (MO-MDSCs, $CD11b^{+}ly6G^{-}ly6C^{hi}$) expressed CCR1 (Fig. 7A), suggesting that the increased expression of CCL9 in the spleen of TB mice may attract MDSCs in a CCR1-dependent manner. Of note, the expression of CCR1 on MO-MDSCs in TB mice was higher compared with that in normal mice, while such a difference was not observed for G-MDSCs (Fig. 7B).

Splenic macrophages produce elevated levels of CCL9 in tumor-bearing mice. Next, it was determined which splenic cells secrete CCL9. CCL9 may be secreted by mononuclear phagocytic cells (34). It was examined whether macrophages were the source of CCL9 in spleen of TB mice. Splenic macrophages ($CD11b^{+}/F4/80^{+}$) from untreated and TB mice were isolated by fluorescence-assisted cell sorting (Fig. 8A) and the expression levels of CCL9 were detected by RT-qPCR. Splenic

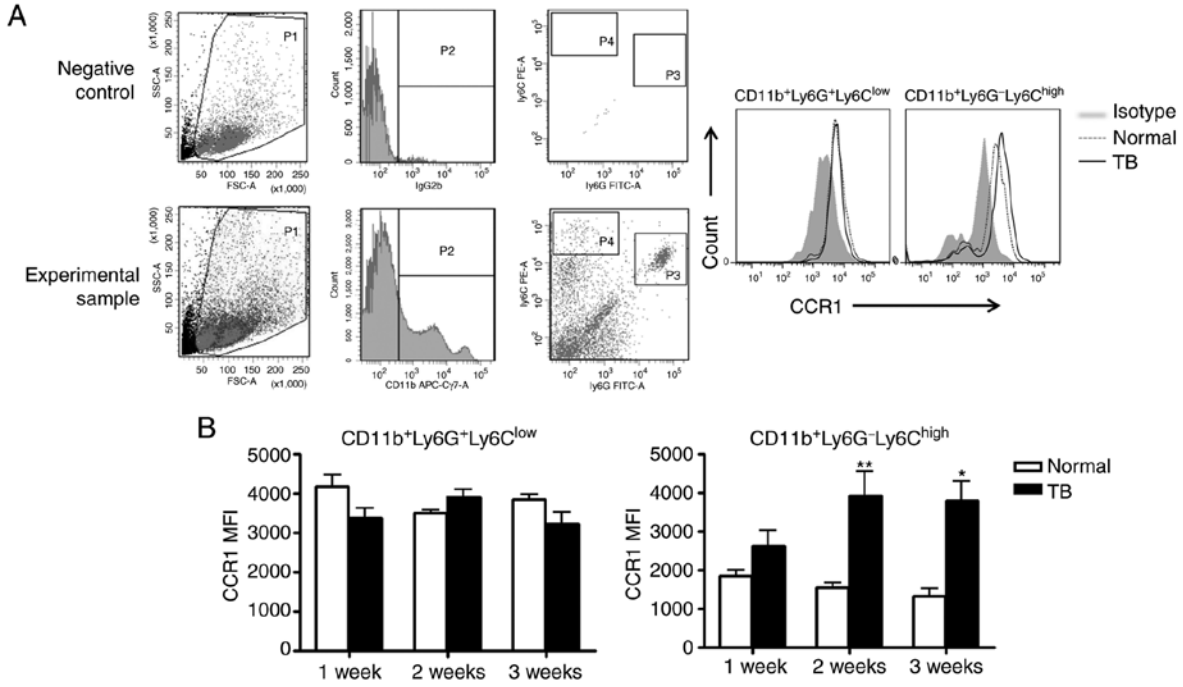

Figure 7. Splenic MDSCs express CCR1, the receptor for chemokine (C-C motif) ligand 9. Splenic single-cell suspensions were stained with anti-mouse ly6G monoclonal antibody conjugated with FITC, anti-mouse ly6C monoclonal antibody conjugated with PE, anti-mouse CD11b monoclonal antibody conjugated with APC-Cy7 and anti-mouse CCR1 monoclonal antibody conjugated with APC. (A) Representative flow cytometry plots and gating strategy. Left panel: A live gate P1 was set in the FSC/SSC plot and CD11b$^+$ cells were included in further analysis with gate P2 (APC/Cy7 rat immunoglobulin G2b, κ isotype antibody was used as the negative control for the separation of negative and positive cell populations). Subsequently, the selected cells were displayed in a histogram for ly6C-PE and ly6G-FITC. The population of CD11b$^+$ly6G$^+$ly6C^{low} cells refers to G-MDSCs, and the population of CD11b$^+$ly6G$^-$ly6C^{high} cells refers to MO-MDSCs. Right panel: Representative plots for the expression of CCR1 on G-MDSCs and MO-MDSCs from the spleen of normal and TB mice. (B) The MFI of CCR1 on G-MDSCs (left panel) and MO-MDSCs (right panel) from H22 hepatoma and normal mice (n=6). Values are expressed as the mean ± standard deviation. *P<0.05 and **P<0.01. TB, tumor-bearing; G-MDSCs, granulocytic myeloid-derived suppressor cells; MO-MDSCs, monocytic MDSCs; TB, tumor-bearing; APC, allophycocyanine; FITC, fluorescein isothiocyanate; PE, phycoerythrin; SSC, side scatter; FSC, forward scatter; MFI, mean fluorescent intensity; CCR1, C-C motif chemokine receptor 1; Cy, cyanine.

macrophages from TB mice produced higher levels of CCL9 than control macrophages at weeks 1, 2 and 3 (Fig. 8B). These results suggest that macrophages may be the source of CCL9 the in the spleen of H22 hepatoma mice.

Discussion

Previous studies have reported that the frequencies of MDSCs increased not only in tumor tissue but also in the spleen of TB mice (12,24,35). The accumulation of splenic MDSCs in TB mice may be caused by their increased proliferation, decreased apoptosis or enhanced chemotaxis to the spleen. In the present study, all three aspects were investigated.

It remains elusive whether the proliferation of MDSCs occurs mainly in the bone marrow or in the spleen. The spleen is the major site of MDSC proliferation in the 4T1 mammary cancer model, and the expansion of splenic MDSCs was caused by their increased survival and decreased apoptosis (36). By contrast, in murine 3LL lung cancer, B16 melanomas and Meth A fibrosarcomas, the proliferation of MDSCs primarily occurs in the bone marrow and not in the peripheral blood, the spleen or the tumor tissue (37). Therefore, in the murine H22 orthotopic hepatoma model of the present study, changes in splenic MDSC proliferation and apoptosis were first assessed. It was identified that the expansion of splenic MDSCs was not associated with their proliferation or apoptosis.

Next, the mechanisms of MDSCs recruitment to the spleen were assessed. In the murine MCA203 fibrosarcoma model, nestin-positive splenocytes are able to secrete CCL2, which caused an elevated level of CCL2 in the spleen and induced MDSC accumulation in the spleen via CCR2 (29). In the present H22 hepatoma model, it was investigated which factor is able to attract MDSCs to the spleen by screening for 62 cytokines. The cytokine protein array and ELISA results revealed that the CCL9 chemokine was highly expressed in the spleen of TB mice.

The overexpressed CCL9 exerts its chemotactic function through binding to its receptor CCR1. Therefore, it was next determined whether MDSCs expressed CCR1. The splenic MDSCs (including G-MDSCs and MO-MDSCs) from normal and TB mice were identified to express CCR1. This indicates that the recruitment of MDSCs to the spleen of TB mice was driven by increases of CCL9 as well as its receptor CCR1, leading to the accumulation of MDSCs in the spleen.

It was then investigated which cell type in the spleen secretes CCL9 in TB mice. CCL9 may be secreted by macrophages, DCs, Langerhans cells, gliocytes, osteoclasts and certain types of tumor cell, including intestinal cancer cells. MDSCs may also be a source of CCL9 (38-40). As the percentage of macrophages in the spleen is higher than that of DCs (35,41,42), the expression of CCL9 in macrophages was examined and it was revealed that splenic macrophages from

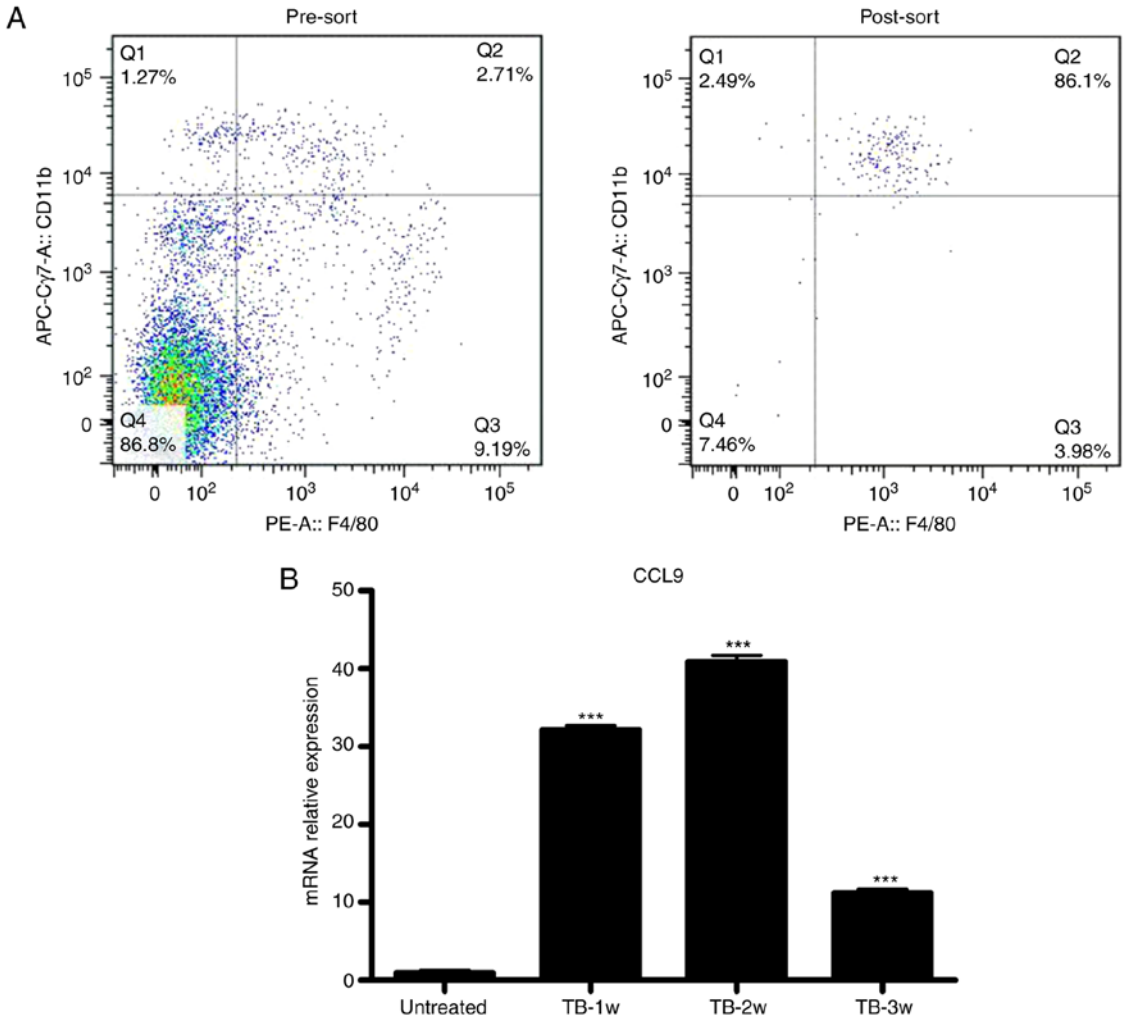

Figure 8. Splenic macrophages produce elevated levels of CCL9 in H22 hepatoma mice. (A) Single-cell suspensions of splenocytes were stained with anti-mouse F4/80 monoclonal antibody conjugated with PE and anti-mouse CD11b monoclonal antibody conjugated with APC-Cy7. The double-positive cells refer to splenic macrophages. Splenic macrophages from untreated and TB mice were isolated by fluorescence-assisted cell sorting. (B) Total RNA was extracted from the sorted splenic macrophages, and the expression of CCL9 relative to GAPDH was examined by reverse transcription-quantitative polymerase chain reaction analysis. ***P<0.001 compared with splenic macrophages from untreated mice. TB, tumor-bearing; 1w, 1 week; APC, allophycocyanine; Cy, cyanine; PE, phycoerythrin; Q, quadrant; CCL9, chemokine (C-C motif) ligand 9.

TB mice had significantly elevated levels of CCL9 compared with those in normal mice. Therefore, it was concluded that the elevated CCL9 secreted by splenic macrophages attracted MDSCs to the spleen of TB mice.

In the H22 orthotopic hepatoma model, a reduction in spleen weight from week 2 to week 3 was previously observed (12). The total number of splenocytes, including macrophages, may decrease at week 3. Macrophages viability and activity may decrease, resulting in reduced cytokine secretion (43). This may explain for the lower expression of CCL9 in the spleen and reduced recruitment of MDSCs to the spleen at week 3 compared with that at week 2.

In conclusion, the results of the present study suggest that in the H22 hepatoma model, splenic macrophages secreted CCL9 that induced MDSC accumulation in the spleen in a CCR1-dependent manner. Further studies should assess which other splenocytes, including DCs or MDSCs, secrete CCL9, whether the mobilization of MDSCs to the spleen may be inhibited by targeting CCL9 or CCR1, and how such an inhibition may affect tumor growth.

Acknowledgements

The authors would like to thank Professor Malgorzata A. Garstka (Core Research Lab of the Second Affiliated Hospital of Xi'an Jiaotong University, Xi'an, China) for critical reading of the manuscript.

Funding

This work was supported by the Program for Changjiang Scholars and Innovative Research Teams at University (grant no. 1171), the National Natural Science Foundation of China (grant no. 81001309) and the Key Research and Development Program of Shaanxi Province of China (grant no. 2017ZDCXL-SF-02-05, 2018SF-197).

Availability of data and materials

All data generated and analyzed during this study are included in this manuscript.

Authors' contributions

BL performed the experiments and wrote the first draft of the manuscript. NH, HC and PW assisted in the establishment of the tumor model and the sample preparation of flow cytometry. SZ assisted in the statistical analysis and data interpretation. JY and ZL designed the study and supervised the experimental work. All authors reviewed the manuscript prior to its submission and approved the final manuscript.

Ethics approval and consent to participate

All animal procedures complied with the Guide for the Care and Use of Laboratory Animals (NIH Publication, 1996) and were approved by the Animal Care and Use Committee of Xi'an Jiaotong University (Xi'an, China).

Patient consent for publication

Not applicable.

Competing interests

The authors declare that they have no competing interests.

References

1. Talmadge JE and Gabrilovich DI: History of myeloid-derived suppressor cells. Nat Rev Cancer 13: 739-752, 2013.
2. Schrader J: The role of MDSCs in hepatocellular carcinoma-in vivo veritas? J Hepatol 59: 921-923, 2013.
3. Kumar V, Patel S, Tcyganov E and Gabrilovich DI: The nature of myeloid-derived suppressor cells in the tumor microenvironment. Trends Immunol 37: 208-220, 2016.
4. Arina A and Bronte V: Myeloid-derived suppressor cell impact on endogenous and adoptively transferred T cells. Curr Opin Immunol 33: 120-125, 2015.
5. Pan PY, Ma G, Weber KJ, Ozao-Choy J, Wang G, Yin B, Divino CM and Chen SH: Immune stimulatory receptor CD40 is required for T-cell suppression and T regulatory cell activation mediated by myeloid-derived suppressor cells in cancer. Cancer Res 70: 99-108, 2010.
6. Gabrilovich DI: Myeloid-derived suppressor cells. Cancer Immunol Res 5: 3-8, 2017.
7. Pardoll DM: Distinct mechanisms of tumor resistance to NK killing: Of mice and men. Immunity 42: 605-606, 2015.
8. You TG, Wang HS, Yang JH, Qian QJ, Fan RF and Wu MC: Transfection of IL-2 and/or IL-12 genes into spleen in treatment of rat liver cancer. World J Gastroenterol 10: 2190-2194, 2004.
9. Imai S, Nio Y, Shiraishi T, Tsubono M, Morimoto H, Tseng CC, Kawabata K, Masai Y and Tobe T: Effects of splenectomy on pulmonary metastasis and growth of SC42 carcinoma transplanted into mouse liver. J Surg Oncol 47: 178-187, 1991.
10. Zusman I, Kossoy G and Ben-Hur H: T cell kinetics and apoptosis in immune organs and mammary tumors of rats treated with cyclophosphamide and soluble tumor-associated antigens. In Vivo 16: 567-576, 2002.
11. Cortez-Retamozo V, Etzrodt M, Newton A, Rauch PJ, Chudnovskiy A, Berger C, Ryan RJ, Iwamoto Y, Marinelli B, Gorbatov R, *et al*: Origins of tumor-associated macrophages and neutrophils. Proc Natl Acad Sci USA 109: 2491-2496, 2012.
12. Li B, Zhang S, Huang N, Chen H, Wang P, Li J, Pu Y, Yang J and Li Z: Dynamics of the spleen and its significance in a murine H22 orthotopic hepatoma model. Exp Biol Med 241: 863-872, 2016.
13. Levy L, Mishalian I, Bayuch R, Zolotarov L, Michaeli J and Fridlender ZG: Splenectomy inhibits non-small cell lung cancer growth by modulating anti-tumor adaptive and innate immune response. Oncoimmunology 4: e998469, 2015.
14. Serafini P, Carbley R, Noonan KA, Tan G, Bronte V and Borrello I: High-dose granulocyte-macrophage colony-stimulating factor-producing vaccines impair the immune response through the recruitment of myeloid suppressor cells. Cancer Res 64: 6337-6343, 2004.
15. Waight JD, Hu Q, Miller A, Liu S and Abrams SI: Tumor-derived G-CSF facilitates neoplastic growth through a granulocytic myeloid-derived suppressor cell-dependent mechanism. PLoS One 6: e27690, 2011.
16. Markiewski MM, DeAngelis RA, Benencia F, Ricklin-Lichtsteiner SK, Koutoulaki A, Gerard C, Coukos G and Lambris JD: Modulation of the antitumor immune response by complement. Nat Immunol 9: 1225-1235, 2008.
17. Shields JD, Kourtis IC, Tomei AA, Roberts JM and Swartz MA: Induction of lymphoidlike stroma and immune escape by tumors that express the chemokine CCL21. Science 328: 749-752, 2010.
18. Yu F, Shi Y, Wang J, Li J, Fan D and Ai W: Deficiency of Kruppel-like factor KLF4 in mammary tumor cells inhibits tumor growth and pulmonary metastasis and is accompanied by compromised recruitment of myeloid-derived suppressor cells. Int J Cancer 133: 2872-2883, 2013.
19. Zhou Y and Guo F: A selective sphingosine-1-phosphate receptor 1 agonist SEW-2871 aggravates gastric cancer by recruiting myeloid-derived suppressor cells. J Biochem 163: 77-83, 2018.
20. Chang AL, Miska J, Wainwright DA, Dey M, Rivetta CV, Yu D, Kanojia D, Pituch KC, Qiao J, Pytel P, *et al*: CCL2 produced by the glioma microenvironment is essential for the recruitment of regulatory T cells and myeloid-derived suppressor cells. Cancer Res 76: 5671-5682, 2016.
21. Blattner C, Fleming V, Weber R, Himmelhan B, Altevogt P, Gebhardt C, Schulze TJ, Razon H, Hawila E, Wildbaum G, *et al*: $CCR5^+$ myeloid-derived suppressor cells are enriched and activated in melanoma lesions. Cancer Res 78: 157-167, 2018.
22. Yamamoto T, Kawada K, Itatani Y, Inamoto S, Okamura R, Iwamoto M, Miyamoto E, Chen-Yoshikawa TF, Hirai H, Hasegawa S, *et al*: Loss of SMAD4 promotes lung metastasis of colorectal cancer by accumulation of $CCR1^+$ tumor-associated neutrophils through CCL15-CCR1 axis. Clin Cancer Res 23: 833-844, 2017.
23. Long X, Ye Y, Zhang L, Liu P, Yu W, Wei F, Ren X and Yu J: IL-8, a novel messenger to cross-link inflammation and tumor EMT via autocrine and paracrine pathways (Review). Int J Oncol 48: 5-12, 2016.
24. Kapanadze T, Gamrekelashvili J, Ma C, Chan C, Zhao F, Hewitt S, Zender L, Kapoor V, Felsher DW, Manns MP, *et al*: Regulation of accumulation and function of myeloid derived suppressor cells in different murine models of hepatocellular carcinoma. J Hepatol 59: 1007-1013, 2013.
25. Bunt SK, Yang L, Sinha P, Clements VK, Leips J and Ostrand-Rosenberg S: Reduced inflammation in the tumor microenvironment delays the accumulation of myeloid-derived suppressor cells and limits tumor progression. Cancer Res 67: 10019-10026, 2007.
26. Sinha P, Clements VK, Fulton AM and Ostrand-Rosenberg S: Prostaglandin E2 promotes tumor progression by inducing myeloid-derived suppressor cells. Cancer Res 67: 4507-4513, 2007.
27. Eisenblaetter M, Flores-Borja F, Lee JJ, Wefers C, Smith H, Hueting R, Cooper MS, Blower PJ, Patel D, Rodriguez-Justo M, *et al*: Visualization of tumor-immune interaction-target-specific imaging of S100A8/A9 reveals pre-metastatic niche establishment. Theranostics 7: 2392-2401, 2017.
28. Ba H, Li B, Li X, Li C, Feng A, Zhu Y, Wang J, Li Z and Yin B: Transmembrane tumor necrosis factor-α promotes the recruitment of MDSCs to tumor tissue by upregulating CXCR4 expression via TNFR2. Int Immunopharmacol 44: 143-152, 2017.
29. Ugel S, Peranzoni E, Desantis G, Chioda M, Walter S, Weinschenk T, Ochando JC, Cabrelle A, Mandruzzato S and Bronte V: Immune tolerance to tumor antigens occurs in a specialized environment of the spleen. Cell Rep 2: 628-639, 2012.
30. Schmittgen TD and Livak KJ: Analyzing real-time PCR data by the comparative C(T) method. Nat Protoc 3: 1101-1108, 2008.
31. Xu P, He H, Gu Y, Wang Y, Sun Z, Yang L and Miao C: Surgical trauma contributes to progression of colon cancer by down-regulating CXCL4 and recruiting MDSCs. Exp Cell Res 370: 692-698, 2018.
32. Vandercappellen J, Van Damme J and Struyf S: The role of the CXC chemokines platelet factor-4 (CXCL4/PF-4) and its variant (CXCL4L1/PF-4var) in inflammation, angiogenesis and cancer. Cytokine Growth Factor Rev 22: 1-18, 2011.

33. Wang Z and Huang H: Platelet factor-4 (CXCL4/PF-4): An angiostatic chemokine for cancer therapy. Cancer Lett 331: 147-153, 2013.
34. Youn BS, Jang IK, Broxmeyer HE, Cooper S, Jenkins NA, Gilbert DJ, Copeland NG, Elick TA, Fraser MJ Jr and Kwon BS: A novel chemokine, macrophage inflammatory protein-related protein-2, inhibits colony formation of bone marrow myeloid progenitors. J Immunol 155: 2661-2667, 1995.
35. Clark CE, Hingorani SR, Mick R, Combs C, Tuveson DA and Vonderheide RH: Dynamics of the immune reaction to pancreatic cancer from inception to invasion. Cancer Res 67: 9518-9527, 2007.
36. Younos IH, Dafferner AJ, Gulen D, Britton HC and Talmadge JE: Tumor regulation of myeloid-derived suppressor cell proliferation and trafficking. Int Immunopharmacol 13: 245-256, 2012.
37. Sawanobori Y, Ueha S, Kurachi M, Shimaoka T, Talmadge JE, Abe J, Shono Y, Kitabatake M, Kakimi K, Mukaida N, *et al*: Chemokine-mediated rapid turnover of myeloid-derived suppressor cells in tumor-bearing mice. Blood 111: 5457-5466, 2008.
38. Lean JM, Murphy C, Fuller K and Chambers TJ: CCL9/MIP-1gamma and its receptor CCR1 are the major chemokine ligand/receptor species expressed by osteoclasts. J Cell Biochem 87: 386-393, 2002.
39. Yan HH, Jiang J, Pang Y, Achyut BR, Lizardo M, Liang X, Hunter K, Khanna C, Hollander C and Yang L: CCL9 induced by TGFβ signaling in myeloid cells enhances tumor cell survival in the premetastatic organ. Cancer Res 75: 5283-5298, 2015.
40. Kitamura T, Fujishita T, Loetscher P, Revesz L, Hashida H, Kizaka-Kondoh S, Aoki M and Taketo MM: Inactivation of chemokine (C-C motif) receptor 1 (CCR1) suppresses colon cancer liver metastasis by blocking accumulation of immature myeloid cells in a mouse model. Proc Natl Acad Sci USA 107: 13063-13068, 2010.
41. Fujimi S, Lapchak PH, Zang Y, MacConmara MP, Maung AA, Delisle AJ, Mannick JA and Lederer JA: Murine dendritic cell antigen-presenting cell function is not altered by burn injury. J Leukoc Biol 85: 862-870, 2009.
42. Gatto D, Wood K, Caminschi I, Murphy-Durland D, Schofield P, Christ D, Karupiah G and Brink R: The chemotactic receptor EBI2 regulates the homeostasis, localization and immunological function of splenic dendritic cells. Nat Immunol 14: 446-453, 2013.
43. Zhang S, Li ZF, Pan D, Huang C, Zhou R and Liu ZW: Changes of splenic macrophage during the process of liver cancer induced by diethylnitrosamine in rats. Chin Med J 122: 3043-3047, 2009.